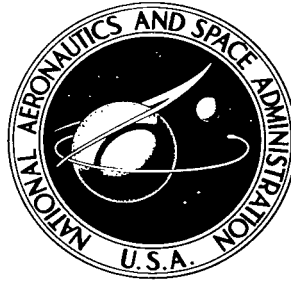


NASA TECHNICAL NOTE



NASA TN D-4078

6.1

NASA TN D-4078

LOAN COPY: RETI
AFWL (WLIL-
KIRTLAND AFB, N



TECH LIBRARY KAFB, NM

AN EVALUATION OF SEA SURFACE TEMPERATURE AS MEASURED BY THE NIMBUS I HIGH RESOLUTION INFRARED RADIOMETER

by Lewis J. Allison and James S. Kennedy

Goddard Space Flight Center

Greenbelt, Md.



AN EVALUATION OF SEA SURFACE TEMPERATURE AS MEASURED
BY THE NIMBUS I HIGH RESOLUTION INFRARED RADIOMETER

By Lewis J. Allison and
James S. Kennedy, Capt. USAF

Goddard Space Flight Center
Greenbelt, Md.

NATIONAL AERONAUTICS AND SPACE ADMINISTRATION

For sale by the Clearinghouse for Federal Scientific and Technical Information
Springfield, Virginia 22151 - CFSTI price \$3.00

ABSTRACT

An analysis of Nimbus I HRIR data over various parts of the world indicated limited success in deriving sea surface temperatures to within 3° to 6°K of aircraft radiation measurements (8-13 μ) and synoptic-climatological ship sea surface temperature data. The areas studied included the east, west and Gulf coasts of the United States, West Greenland, Nova Scotia, southern Japan, the eastern Mediterranean Sea, Caspian Sea, Persian Gulf, and the Indian Ocean. At night, thin clouds which may fill the radiometer's field of view make it difficult to interpret the absolute values of derived sea surface temperature. During the daytime, the HRIR data is unusable for oceanographic temperature analysis because the contamination by reflected solar radiation mixes with the emitted radiation. Future satellite instrumentation, consisting of a HRIR radiometer (10-11 μ) when used in conjunction with television data, will delineate cloud free ocean areas and permit the daily derivation of sea surface temperatures from approximately 10 to 30% of the world's oceanic regions.

CONTENTS

Abstract	ii
INTRODUCTION	1
METHODS OF OCEANOGRAPHIC ANALYSIS	1
THE NIMBUS I HRIR EXPERIMENT	2
EXAMPLES OF NIMBUS I HRIR ANALYSES OF SEA SURFACE TEMPERATURES	4
Cold Water Regions	4
Warm Water Regions	9
CONCLUSION	23
ACKNOWLEDGMENTS	23
References	23

AN EVALUATION OF SEA SURFACE TEMPERATURE AS MEASURED BY THE NIMBUS I HIGH RESOLUTION INFRARED RADIOMETER

by

Lewis J. Allison and

James S. Kennedy,* Capt. USAF

Goddard Space Flight Center

INTRODUCTION

The feasibility of making meaningful sea surface temperature measurements from space vehicles was discussed in great detail at the Woods Hole Oceanographic Institution, Massachusetts, in August 1964 (Reference 1). It was concluded then and in more recent studies (References 2 and 3) that satellite mapping of sea surface temperatures on a synoptic basis would help answer pressing operational oceanographic questions concerning the large scale dynamic processes of the ocean, the interaction of sea and air during hurricane and extratropical cyclone development, near-shore processes involving fog and sea ice formation, location of major ocean current systems by boundary temperature gradients and the distribution of fish of economic importance.

This study was conducted specifically to evaluate the capability of the Nimbus I satellite to map sea surface temperatures by use of the High Resolution Infrared Radiometer (HRIR) over a wide range of latitudes. Comparisons of nighttime HRIR equivalent blackbody temperatures (T_{BB} in °Kelvin) of the sea surface with aircraft radiometer data and conventional ship sea surface temperatures were made on a near-synoptic and climatological time scale.

METHODS OF OCEANOGRAPHIC ANALYSIS

Ever since the pioneering efforts of the HMS CHALLENGER deep-sea expedition in 1872, there has been an increasing requirement for detailed sea surface temperatures on a global basis. Ewing expressed this opinion at the Third Symposium on Remote Sensing in the Environment, in October 1964 (Reference 4). He also indicated that in the past, data collection in the field of oceanography consisted of the scant information provided by a few ships probing the vertical dimension of the sea. These data were grossly discontinuous in time and space. Many areas of the oceans have never been visited by physical scientists and published charts now show data gathered in widely different years by basically different methods.

*Air Weather Service Member.

Polar orbiting satellites with newly developed infrared sensors can increase the frequency, range and density of these oceanographic observations. The ultimate oceanographic requirement is for daily global sea surface temperature observations on a 50-mile or less grid spacing. One hundred mile spacing or weekly intervals is the limit of acceptability. The optimum satellite coverage should show the real sea surface temperature in an area 25 miles or less within an accuracy of $\pm 0.5^{\circ}\text{C}$. All data should be corrected for diurnal heating and cooling and atmospheric absorption.

During the years 1962-1964, several U. S. government agencies undertook the monthly survey of sea surface temperature by research aircraft along the Atlantic, Pacific, and Gulf coasts of the United States (Reference 5). Measurements were recorded by infrared radiometers at an altitude of a few hundred feet along fixed flight paths. One of the major factors affecting the measurement of absolute sea surface temperatures by aircraft radiometers is the loss due to atmospheric absorption by water vapor at low altitudes. Corrected aircraft infrared data have proved valuable to the Bureau of Commercial Fisheries, and the U. S. Navy, Antisubmarine Warfare Program (ASWEPS).

THE NIMBUS I HRIR EXPERIMENT

The Nimbus High Resolution Radiometer consists of a single channel radiometer designed and built by the ITT Laboratories, Fort Wayne, Indiana. It contains a lead selenide (PbSe) photoconductive cell which is space-radiative cooled to -75°C and operates best at night in the 3.5 to 4.1μ "window" region (Figure 1).

The radiometer has an instantaneous field of view of $1/2$ degree which, at an altitude of 930 km, corresponds to a subsatellite resolution of 8 km at the nadir. The Nimbus vertical control system demonstrated an accuracy of 1° which corresponds to a subsatellite position error of 16 km in the location of a scan spot from an altitude of 925 km. On a global basis this is an acceptable error for meteorological analysis. The radiometer is attached to the earth-oriented sensory ring and scans the earth's surface from horizon to horizon, a distance of approximately 2000 km at a scan rate of 44.7 revolutions per minute. During the 99 minute orbit, the radiometer detector alternately views the housing cavity, outer space, and the earth's surface. The outer space level serves as a zero reference and together with the radiometer housing temperature data is telemetered for calibration purposes to the read-out stations at Fairbanks, Alaska, or Rosman, North Carolina.

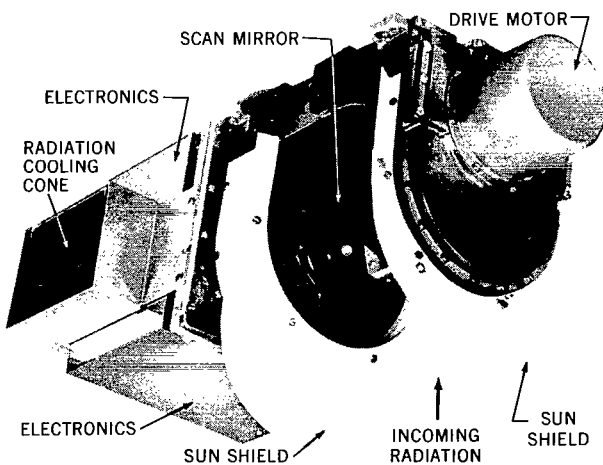


Figure 1—Nimbus I High Resolution Infrared Radiometer.

The range of T_{BB} values lies between 210°K and 330°K with a noise-equivalent temperature difference of 1°K for a 250°K background (Reference 6). Calculations of theoretical values of outgoing radiation for several model atmospheres indicate that the atmospheric absorption due to water vapor and carbon dioxide was much smaller for the HRIR data than for the TIROS 8-12 μ channel 2 "window" data. Sea surface temperatures, recorded by the HRIR under clear sky conditions for the ARDC Standard Atmosphere, for 0° to 75° zenith angles, should be increased by 1.5° to 4.8°K; however, TIROS 8-12 μ data should be increased by 9.2° to 14.9°K for similar conditions. Similarly, the HRIR data should be corrected by +0.3° to 2°K for drier winter high latitudes and +2.3° to 5°K for humid tropical regions at low zenith angles (Reference 7).

Averaged over the entire globe and over twenty-four hours, short-wave radiant energy from the sun impinges 0.5 calories on each horizontal square centimeter per minute at the top of the atmosphere, 0.24 calories of which reach the ocean surface. Most of the latter radiation is absorbed by the top three-foot layer of water; and the heat balance is maintained largely by long wave reradiation from the very top water levels and by evaporative cooling. Since the emissivity of the ocean in the 3.5-4.1 μ regions is approximately 0.98, the infrared characteristics of the ocean surface approach those of a blackbody (Reference 8). Temperature measurements of the shallow surface layer ("cool skin") indicated that this layer was at least 0.6°C cooler than the water at the 15-cm depth. Only a very thin layer of water, 0.06 mm, is required to absorb infrared radiation completely in the 3.5-4.1 μ region (Reference 9). Diurnal corrections up to 0.5°K should be made to measured T_{BB} values of sea surface temperature to compensate for boundary layer cooling at night (Reference 10). The annual climatological variation of sea surface temperature is 15° to 18°F at 50°N in the Atlantic and Pacific Oceans respectively, and 9° to 10°F in the southern hemisphere temperate zone and 3° to 4°F in the tropical oceans.

Since ocean surface temperatures range from -2°C(271°K) to +35°C(308°K) a careful study of Nimbus nighttime orbits was made to cover a wide range of latitudes (Reference 11). During 26 days of Nimbus operation, August 28 - September 23, 1964, radiation data were obtained for about 50 percent of all nighttime orbits from the North Pole to the South Pole. The HRIR measurements made during the daytime hours, however, cannot be used for sea surface temperature analysis without additional corrections because of reflected solar radiation.

The oceans cover approximately 71 percent of the earth's surface, 40 to 60 percent of which is cloud covered. Cloud contamination is a serious problem since it is impossible to confirm the complete absence of nighttime cloud cover over the oceans from conventional weather maps. Low clouds can feign low sea surface temperature especially in areas of upwelling and strong surface mixing, hence greater care is needed in interpreting the radiation data in these regions at night. The darker oceanic regions seen on the Nimbus I photofacsimile film strips were used as a guide to the clear night sky condition. A selection of mercator grid print sea surface temperature maps was printed out by the IBM 7094 computer on a 1:2 million scale. The infrared data, uncorrected for water vapor and CO₂ absorption, nadir angle, or boundary layer cooling, were analyzed for 1°K intervals of equivalent blackbody temperature (T_{BB}). The data contained an average population count of 2 to 10 scan spots for each plotted T_{BB} value on a scale of 0.250

degrees of longitude per mesh interval. In order to avoid space contamination, the maximum scan nadir angle was restricted to the range 69° to 65° depending upon the height of the satellite in the 423 to 932-km range.

EXAMPLES OF NIMBUS I HRIR ANALYSES OF SEA SURFACE TEMPERATURES

Cold Water Regions

West Greenland Current

Two tongues of warm water (40° to 42°F) carried by the West Greenland Current through the Northabout Route and the Middle Passage, usually permit the summertime passage of United States

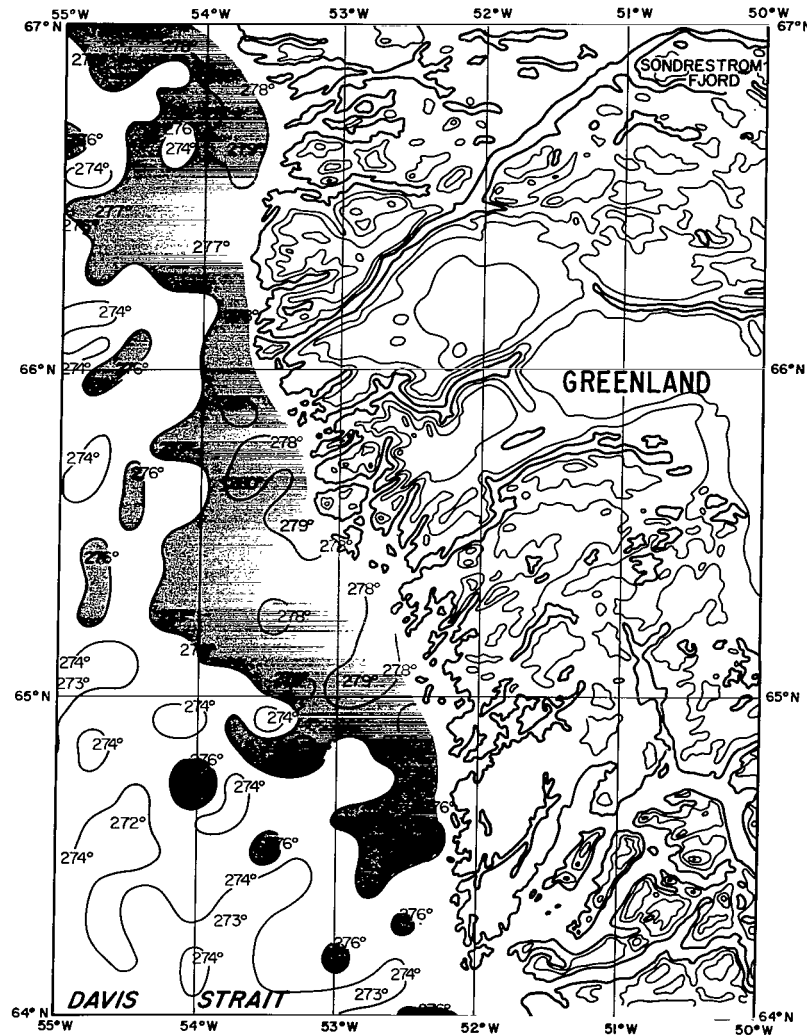


Figure 2—Analysis of HRIR T_{BB} values (°K) from Nimbus I orbit 086 R/O 086, 0455Z for 3 min. on 3 September 1964, over the West Greenland Current.

MSTS resupply vessels to Thule, Greenland. However for the 1964 summer season, the incursion of warm water did not extend as far north as expected. Sea surface temperatures fell 4° to 5°F below normal and a record-breaking ice concentration was noted by ice breakers in Melville Bay, north of 71°N (Reference 12). A search for Nimbus I nighttime data in this arctic region indicated that a relatively clear area off the west Greenland coast near Sondrestrom was worthy of investigation. Figure 2 shows the analyzed HRIR sea surface temperature chart for orbit 086 at 0455Z, 3 September 1964. The major portion of the shaded area encloses the 276° to 279°K (37° to 43°F) isotherms. These T_{BB} values are within 1° to 3°K of the 1964 summer season sea surface temperatures (276° to 277°K) shown in Figure 3. The unshaded area of <276°K was probably cloud contaminated. When a statistical study of the accuracy of U. S. Navy picket ship and

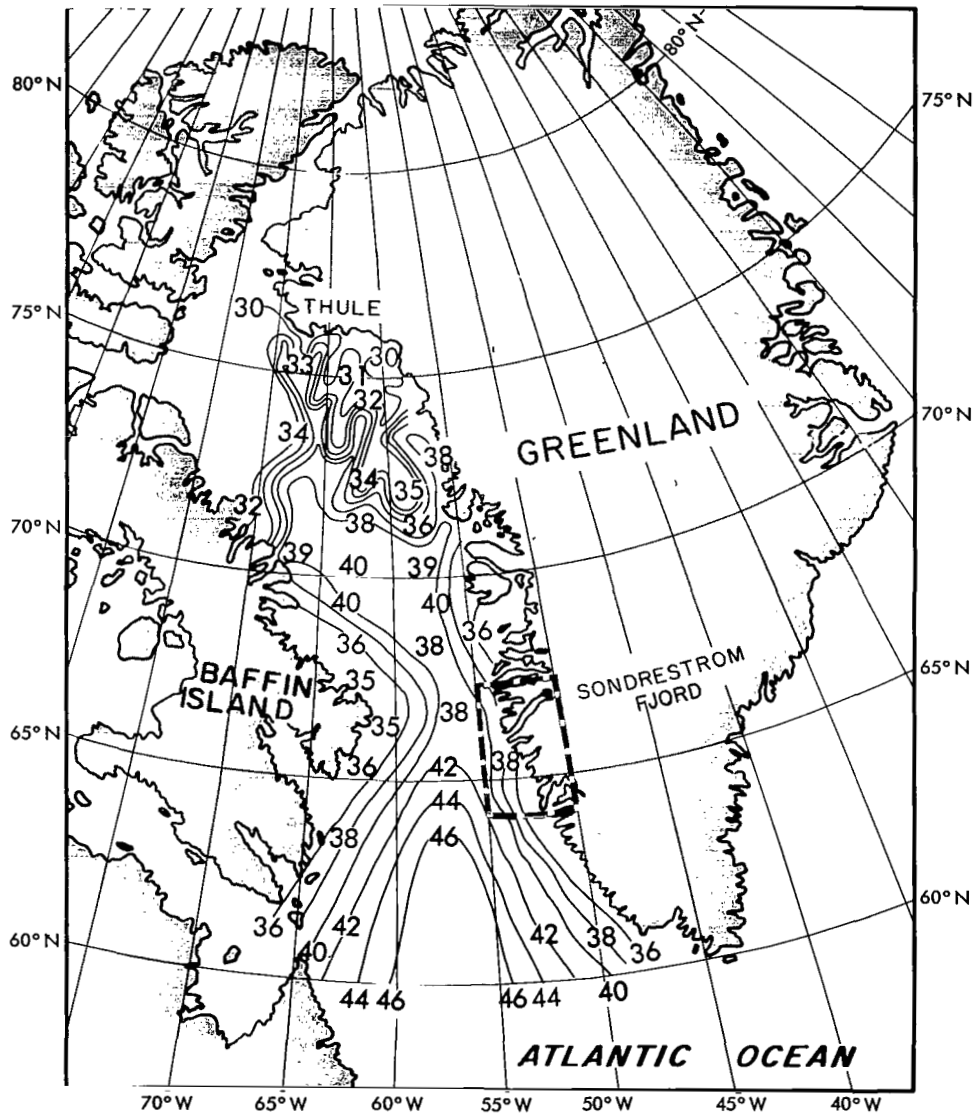


Figure 3—Ship sea surface temperature chart (°F) for the Summer 1964 (May - August) analyzed by the Oceanographic Prediction Division, U. S. Naval Oceanographic Office, Washington, D. C.

MSTS ship sea water injection temperatures was compared with surface temperature observations, the ship intake temperatures were found to be $1.2^{\circ}\text{F} \pm 0.6^{\circ}\text{F}$ colder than the surface temperature for 95% of the observed time (Reference 13). Coupled with the facts that the depth of the water intake level varies with each ship's cargo (10 to 30 feet) and that only a very limited number of ships provided sea surface observations along the West Greenland coast during the 1964 summer and early fall season, the above mentioned small 1° to 3° temperature difference may be the result of the compensation of two errors mentioned above.

The Labrador Current

An understanding of the daily interaction of the Labrador Current with the Gulf Stream could yield significant improvements in synoptic weather forecasts and affect the recently developed

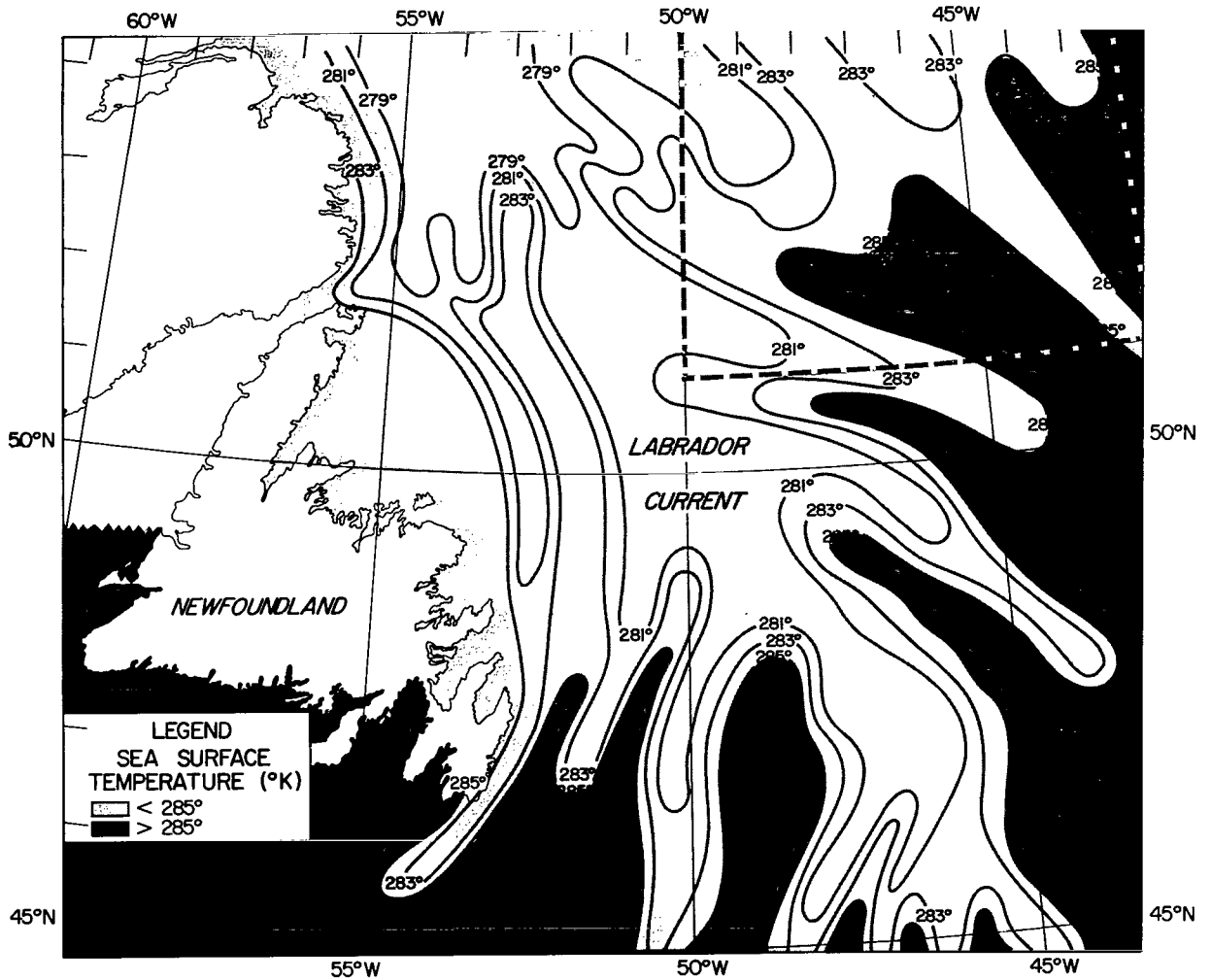


Figure 4—Ship sea surface temperature chart (°K) analyzed by the Canadian Oceanographic Services for September 15, 1964 in the Newfoundland area.

technique of ship routing in the North Atlantic. The sea surface temperatures are closely related to the character of the Labrador Current and the Gulf Stream both of which in turn primarily respond to the prevailing oceanic wind systems. The major sea currents move approximately 45° to the right of the wind direction in the Atlantic Ocean and are influenced by land boundaries along the east coast. Factors which affect the "heat budget" of the sea surface are the regional excess of evaporation or precipitation, the exchange of sensible heat from overriding cold or warm air masses by molecular processes, wind-wave mixing, by convection, and surface friction (Reference 14).

Figure 4 shows the surface water interaction pattern along the southern perimeter of the cold Labrador Current as analyzed by the Canadian Oceanographic Service on September 15, 1964, from all available ship data within the area of interest. The darker shaded area indicates sea surface temperatures higher than 285°K. Figure 5 shows the analyzed HRIR sea surface

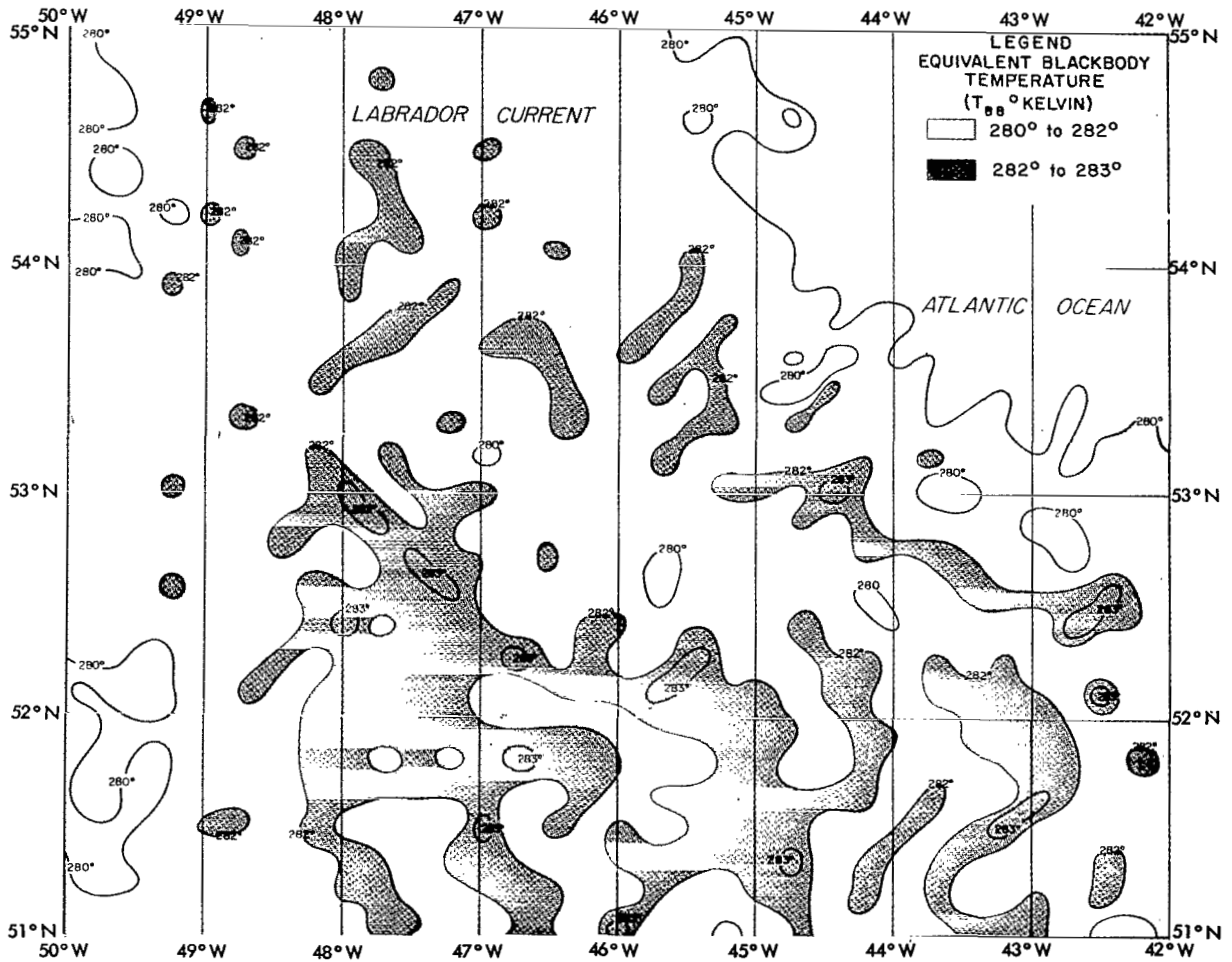


Figure 5—Analysis of HRIR T_{BB} values (°K) from Nimbus I orbit 246 R/O 247, 0326Z for 6 min. on September 14, 1964 east of Newfoundland.

temperature chart for Nimbus orbit 246 at 0326Z, 14 September 1964. The two grey shaded areas enclose the 280° to 283°K (7° to 10°C) isotherms. These values are 1° to 4°K colder than the September 15th ship sea surface temperature data shown in Figure 4. In general the HRIR analysis shows a similarity in the gross temperature gradients and the patterns of cold to warmer water shown in the isothermal analyses provided by the Canadian Oceanographic Service. The satellite radiation data contain at least 200 to 300 times more sea surface temperature information per 1° latitude-longitude square than conventional ship data and, therefore, should depict the sea surface temperature patterns in greater detail.

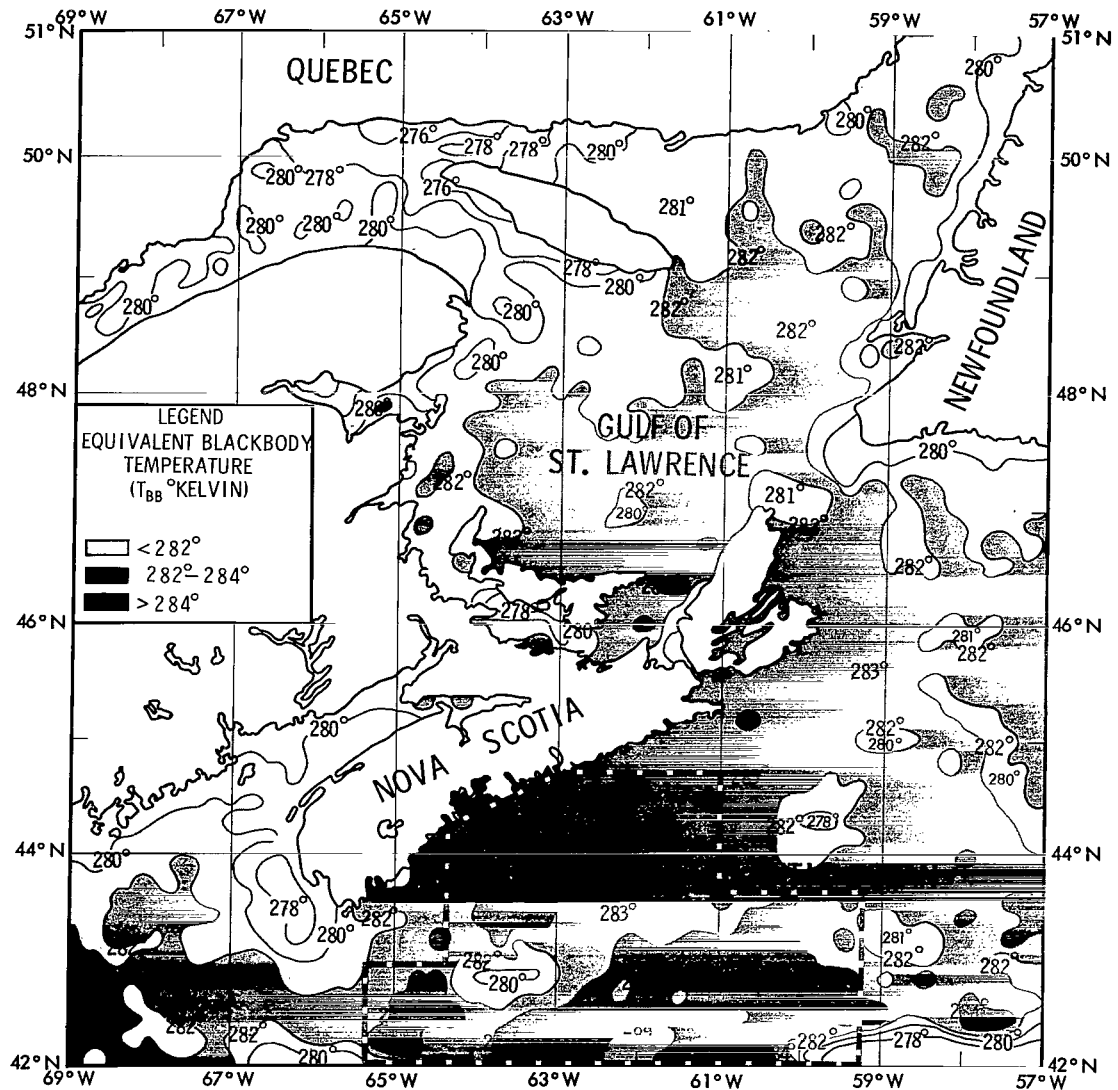


Figure 6—Analysis of HRIR T_{BB} values ($^\circ$ K) from Nimbus I orbit 188 R/O 192, 0418Z for 9 min. on September 10, 1964 off Nova Scotia.

Another example of the sea surface mixing of the southerly moving Labrador Current and the warm Gulf Stream is shown in Figures 6 and 7. Figure 6 shows the analyzed HRIR sea surface temperature chart for orbit 188 at 0418Z, 10 September 1964. The two darker shaded areas enclose areas warmer than 282°K. These values are 5° to 9° K colder than the September 9-13, 1964 ship sea data shown in Figure 7. A uniform sea surface temperature pattern of 50° to 60°F isotherms is shown enclosing Nova Scotia, while extensive meridional mixing of 65° to >80°F water is seen along the north wall of the Gulf Stream as it flows at approximately 2 to 4 kts in a northeasterly direction. Considering the long 5-day period of inter-comparison and the good possibility of nighttime low level cloud contamination in this dynamic mixing zone, the 5° to 9°K temperature differences appear to be reasonable.

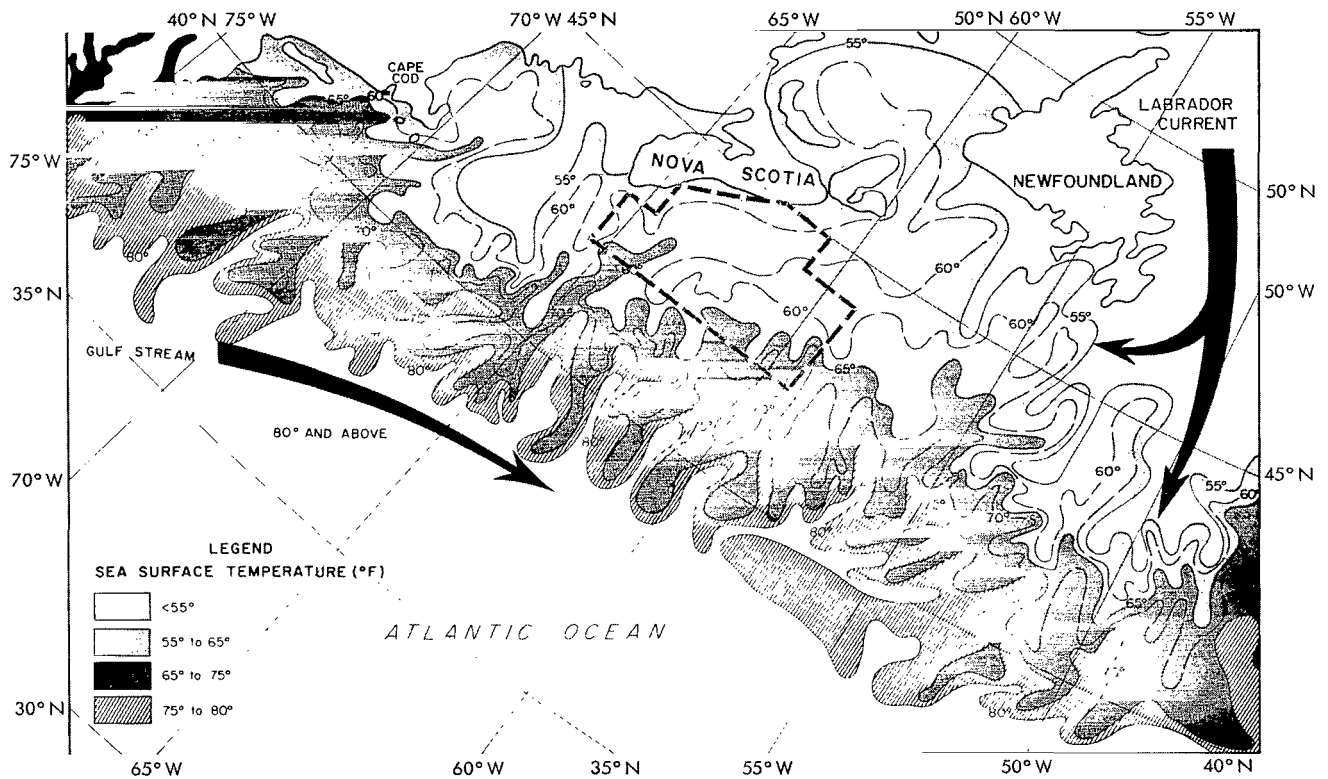


Figure 7—Ship sea surface temperature chart (°F) analyzed by the Oceanographic Prediction Division, U. S. Naval Oceanographic Office, Washington, D. C. for September 9-13, 1964 along the northeast coast of the United States.

Warm Water Regions

The Southern California Coast

One of the most pressing problems in synoptic oceanography is determining the cause of large scale shifts in oceanic surface water masses which in turn affect the weather, fisheries (Reference 15), and underwater sound propagation. An example of such an anomalous current is the "El Nino"

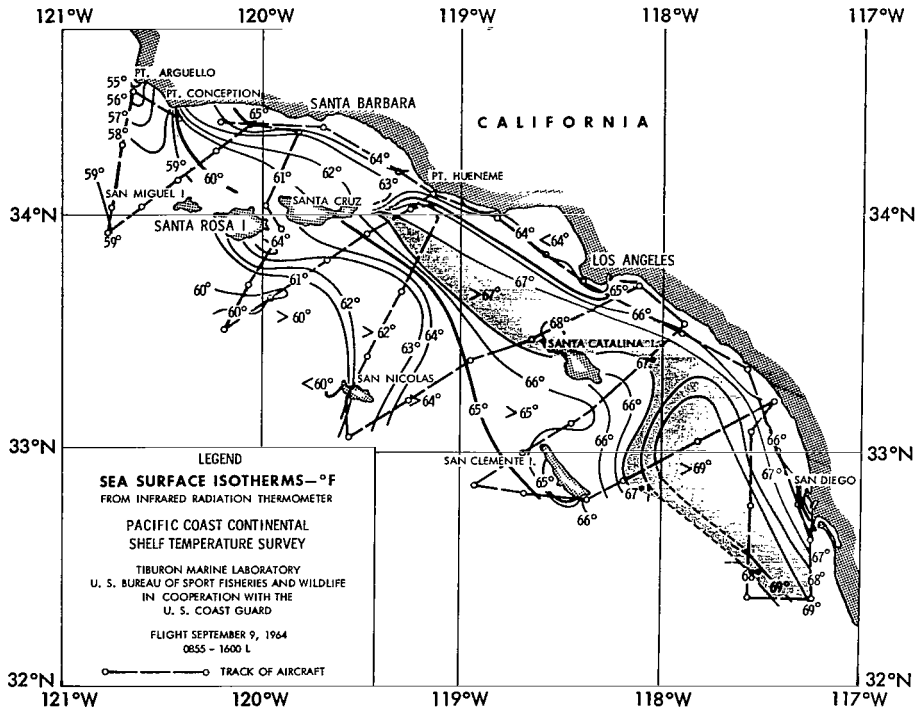


Figure 8—Aerial sea surface temperature survey, from 0855 to 1600L, on September 9, 1964. The flight was conducted by the Tiburon Marine Laboratory, U. S. Bureau of Sport Fisheries and Wildlife in cooperation with the U. S. Coast Guard. Data were recorded by a Barnes IRT (8-13 μ) analyzed in °F.

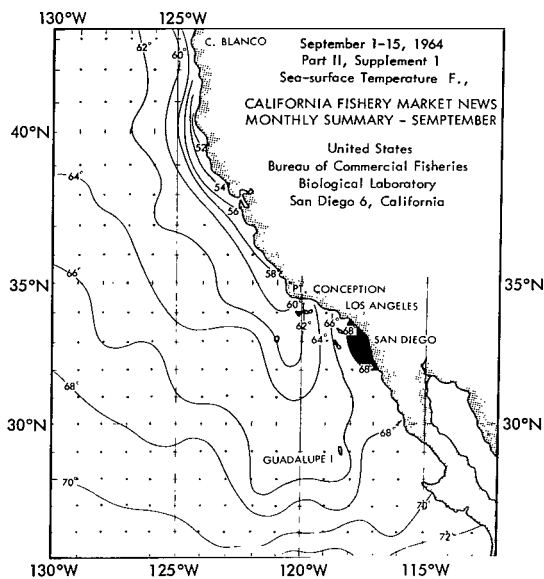


Figure 9—Ship sea surface temperature chart (°F) analyzed by the U. S. Bureau of Commercial Fisheries, Biological Laboratory, California, for September 1-15, 1964, along the west coast of the United States.

which periodically appeared along the coasts of Peru and Ecuador, in 1891, 1925, 1941, 1953, and 1957. Indications have been received of its reappearance in 1965-66 (Reference 16). This southerly-flowing extension of the Equatorial Countercurrent brought unusually high sea surface temperatures to the west coast of South America which resulted in wholesale starvation of fish, mass destruction of the guano birds, and abnormal flooding due to heavy coastal rainfall. Another well-documented large scale shift occurred in the California Current system in the Gulf of Alaska when unusually warm water (6° to 8°F above normal) was recorded in the Fall of 1957 (Reference 17).

In view of the foregoing discussion, a search was made for clear nighttime Nimbus coverage of a warm current in the Eastern Pacific supported by conventional meteorological

data. Figure 8 shows an analysis of "warm" sea surface water enclosed by the shaded area (67° to $>67^{\circ}$, 292° to $>292^{\circ}$ K) off the southern California coast. These data were recorded during an aircraft survey flight from 0855 to 1600L on September 9, 1964 by the U. S. Coast Guard, in cooperation with the Tiburon Marine Laboratory. The aircraft was equipped with a Barnes Infrared Thermometer ($8-13\mu$) and flown under clear sky conditions along the California coast at approximately 500 feet altitude. The T_{BB} values recorded by the aircraft radiometer were corrected by $\pm 0.7^{\circ}\text{F}$ in order to conform to bucket temperatures at the NEL oceanographic tower in the local area. Figure 9 is a conventional ship sea surface temperature chart ($^{\circ}\text{F}$) for the period 1-15 September 1964 along the west coast. This chart, which was prepared and analyzed by the Bureau of Commercial Fisheries, shows a similar "warm" area (68°F - shaded) along the coast between Los Angeles and San Diego. The cooler southerly-flowing California current is indicated along 120°W . HRIR data recorded at night during orbit 073, 0744Z on 2 September 1964 were analyzed, as shown in Figure 10. A similar shaded area of "warm" water (290° to $>290^{\circ}$ K, 63° to $>63^{\circ}\text{F}$) is shown close in to the coastline. These September 2nd HRIR T_{BB} values averaged 2° to 3°K colder than the

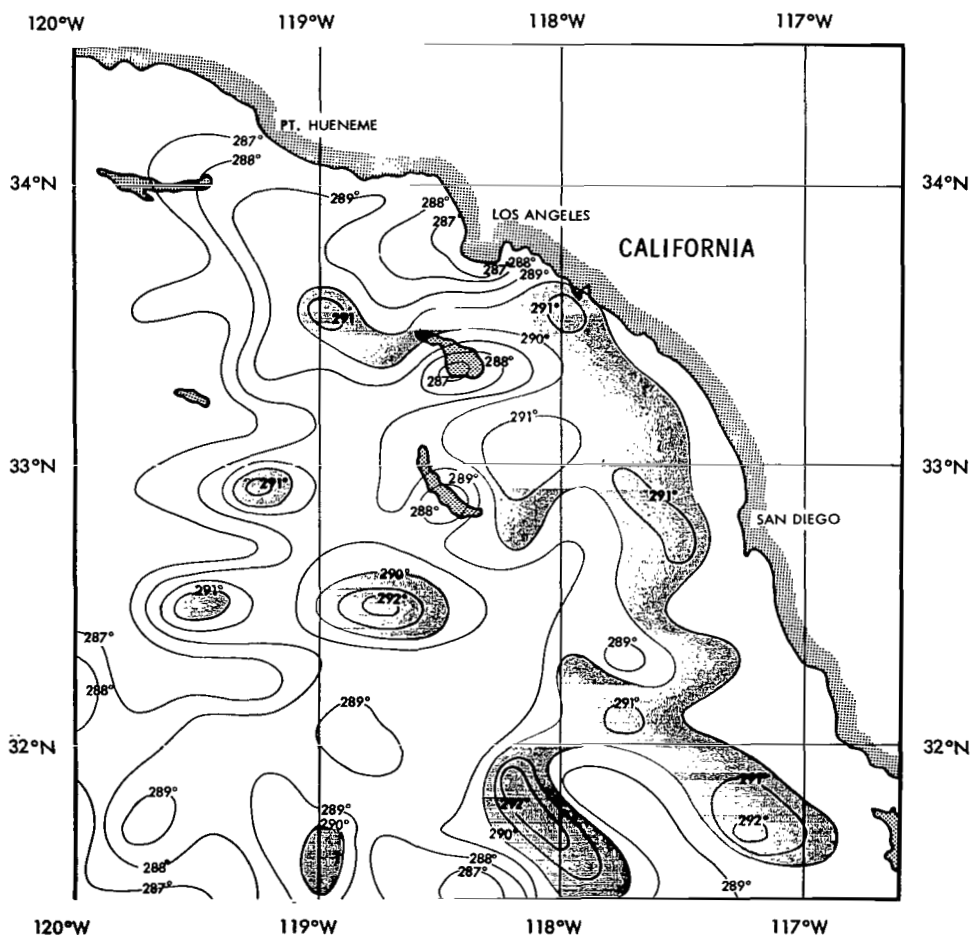


Figure 10—Analysis of HRIR T_{BB} values ($^{\circ}\text{K}$) from Nimbus I orbit 073 R/O 075, 0744Z for 4 min., on 2 September 1964 along the west coast of the United States.

September 9th aircraft radiation values and 3° to 4°K colder than the September 1-15, 1964 averages. The lower T_{BB} values, <291°K, located west of 119°W, were probably caused by low level stratocumulus over-lying the cool upwelled water indicated in Figure 9.

A good example of warm T_{BB} values recorded over a partially land-locked water area is shown during the same orbit in Figure 11. Maximum water T_{BB} values of 298° to >300°K are shown north of 30°N at the head waters of the Gulf of California. Comparative conventional climatological and synoptic ship data were lacking in this area.

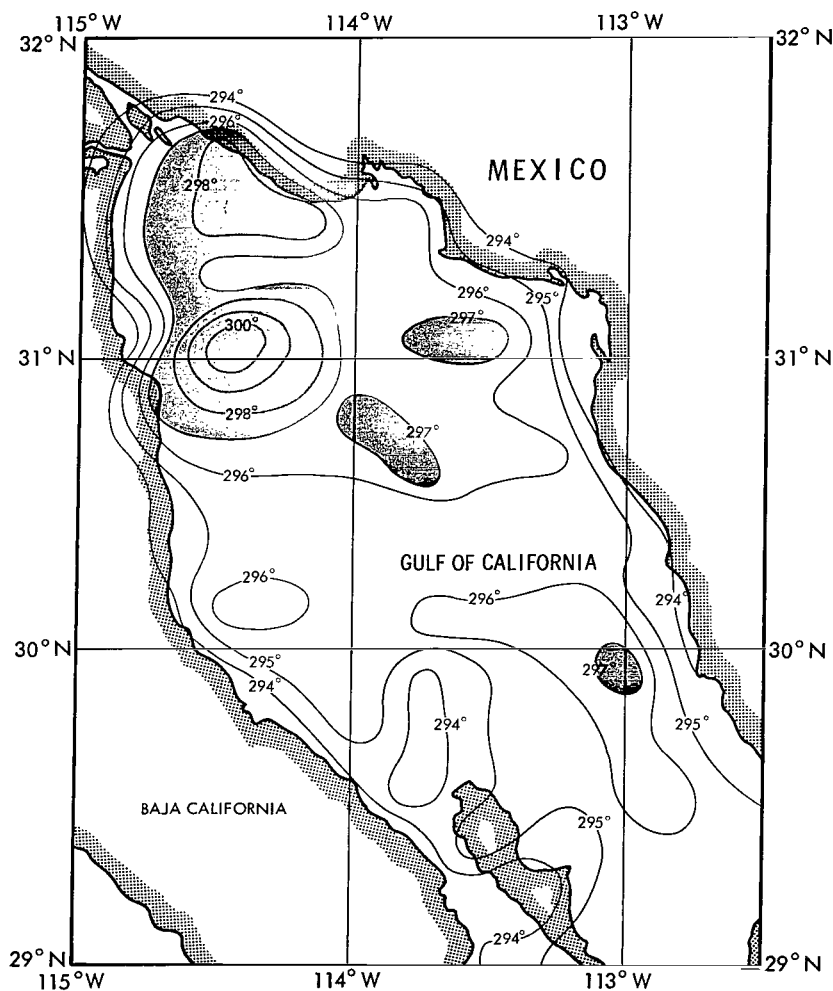


Figure 11—Analysis of HRIR T_{BB} values (°K) from Nimbus I orbit 073 R/O 075, 0744Z for 4 min., on 2 September 1964 over the Gulf of California.

The Gulf Coast

The North Equatorial Current, driven by the Northeast Trade Wind in the Atlantic Ocean, carries a great bulk of water into the Caribbean Sea, and on through to the Gulf of Mexico. From the

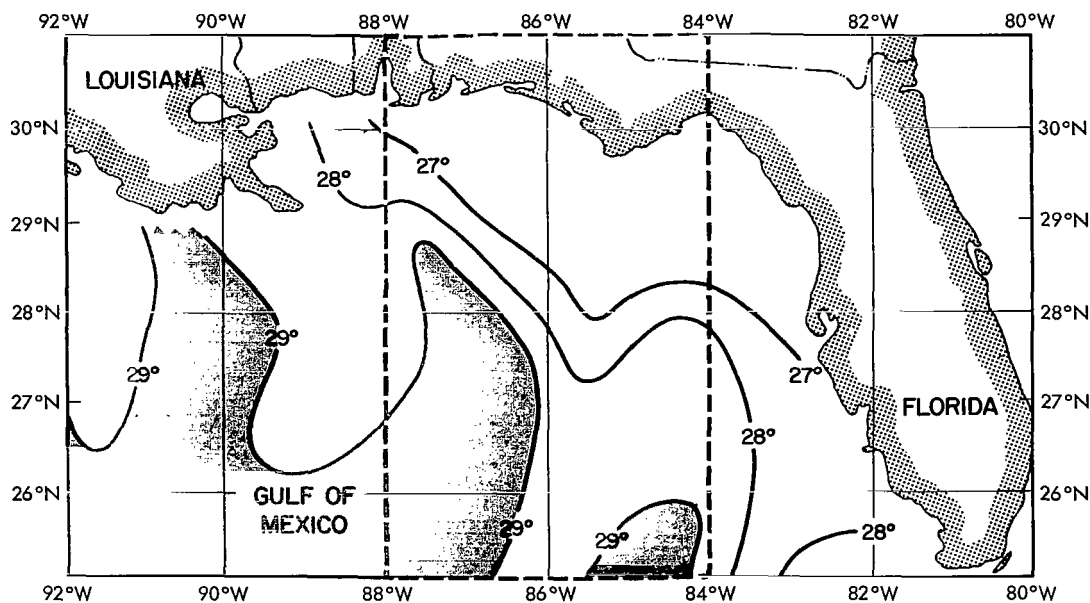


Figure 12—Ship sea surface temperature pattern ($^{\circ}\text{C}$) based upon merchant ship data collected by the U. S. Weather Bureau for September 24–30, 1964 in the Gulf of Mexico, analyzed in Reference 18.

eastern portion of the Gulf; this water flows out through the Straits of Florida as "pulses" of a warm, swift current which converges to form the southern base of the Gulf Stream. The surface water temperature and current pulsation process is of interest to the synoptic oceanographer because of the whiplike undulations of the Gulf Stream. In studying the water temperature of the eastern Gulf, we were fortunate to obtain sea surface temperature observations collected by the U. S. Weather Bureau during September 24–30, 1964 (Figure 12 and Reference 18). Figure 13 shows HRIR data recorded at night during orbit 335 R/O 338 at 0530Z on 20 September 1964. A comparison of these two figures show the HRIR data to be increasing in temperature, north to south, from 294° to 298°K while the ship data increase similarly from 27° to 30°C (300° to 303°K). Figure 14 presents an analysis of aircraft radiation data recorded during a survey flight at 300 feet over the Gulf of Mexico from 0900–1700L, 15–16 September 1964. Comparisons between the aircraft data and bucket temperatures at a research tower near Panama City, Fla. indicated a $\pm 0.7^{\circ}\text{F}$ range of values. The area of comparison lies in the eastern portion of the flight path where T_{BB} values of 80° to 83°F (300° to 301°K) are indicated. The 20 September Nimbus I

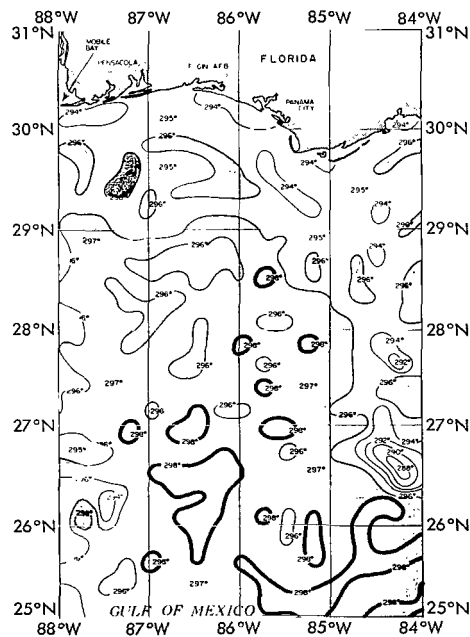


Figure 13—Analysis of HRIR T_{BB} values ($^{\circ}\text{K}$) from Nimbus I orbit 335 R/O 338, 0530Z for 8 min., on 20 September 1964 over the Gulf of Mexico.

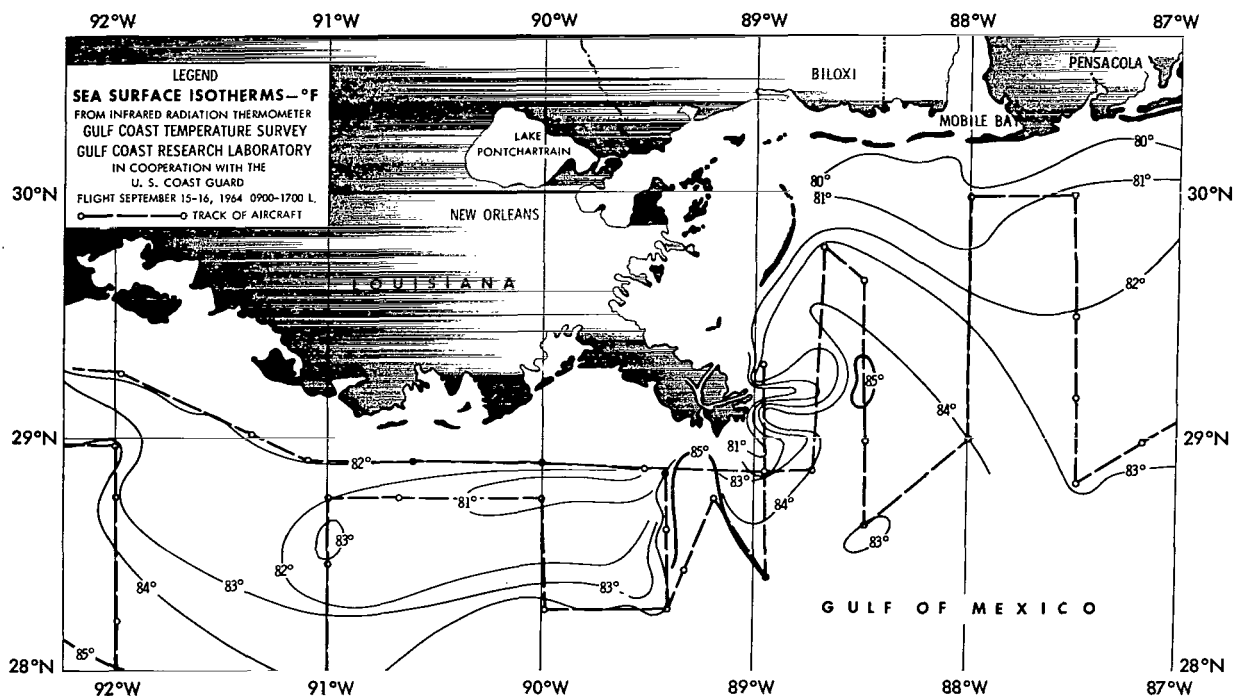


Figure 14—Aerial sea surface temperature survey from 0900-1700L, on 15-16 September 1964. Flight was conducted by the Gulf Coast Research Laboratory, in cooperation with the U.S. Coast Guard. Data were recorded by a Barnes IRT (8-13 μ), analyzed in °F.

values averaged 4° to 6°K colder than the 15-16 September aircraft values and 3° to 5°K colder than the 24-30 September ship sea temperature observations.

The Japanese (Kuroshio) Current

The Kuroshio Current is a strong, permanent warm current similar to the Gulf Stream which is driven by the Pacific High in a northeastward direction from the east coast of Formosa past the southeast coast of Honshu, Japan. Changes in the direction of the current occur during the transitional months of April, May, and September.

Figure 15 shows the HRIR data recorded at night during orbit 136 R/O 139 at 1501Z, on September 6, 1964. The darker shaded areas indicate the warm 297° to 298°K T_{BB} values which lie in the mean flow path of the Kuroshio Current. These T_{BB} values are 4° to 7°K colder than the September climatological mean ship sea temperature data shown in Figure 16.

The Sub-Tropical Atlantic Ocean

The relationship between the life cycle of hurricanes and the sea surface temperature has been studied by Fisher (Reference 19) and Perloth (Reference 20). From these synoptic investigations, it was noted that the hurricanes that generally tend to form in low latitudes

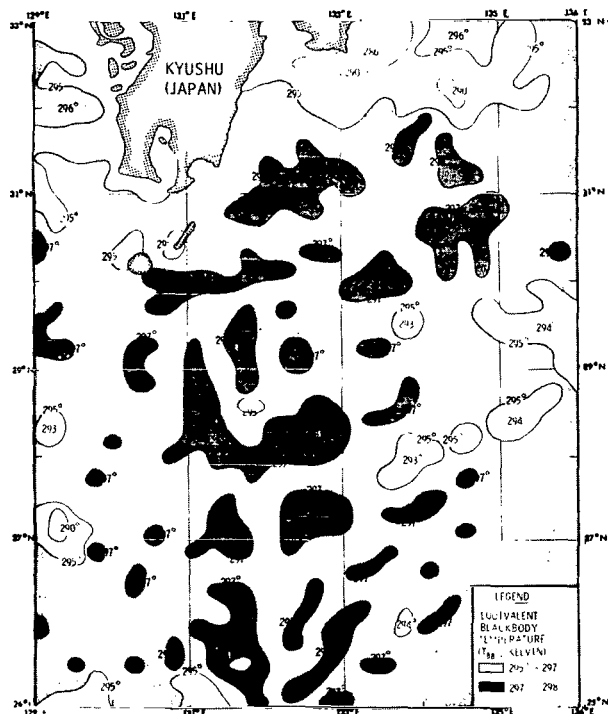


Figure 15—Analysis of HRIR T_{BB} values ($^{\circ}K$) from Nimbus I orbit 136 R/O 139, 1501Z for 9 min., on 6 September 1964 over the Japanese (Kuroshio) Current.

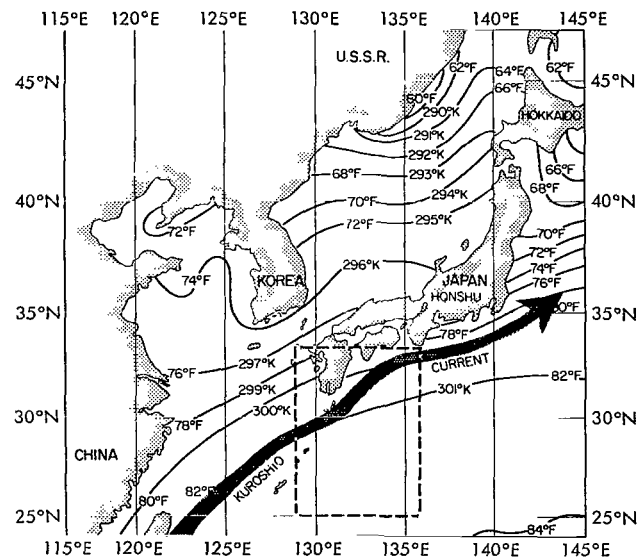


Figure 16—Climatological mean ship sea surface temperature ($^{\circ}F$) chart analyzed by the U.S. Naval Oceanographic Office, Wash., D.C., for September over the Japanese (Kuroshio) Current.

water whose surface temperature was $<79^{\circ}F$. Evidence of marked cooling in the surface layers of the ocean has been noted following intense typhoons in the Pacific (Reference 21) and hurricanes in the Gulf of Mexico and the Atlantic Ocean (References 18 and 19). Warm surface waters were displaced to either side of the cyclone path and a core of cold water appeared near the center of the wake. This intense cooling was confined essentially to a region within twice the radius of the maximum winds (Reference 22).

over warm water (above $83^{\circ}F$) tend to de-intensify when one or more quadrants lay over cooler water (79° to $82^{\circ}F$), and that they fill over

Unfortunately, during the short 26-day operating lifetime of Nimbus I, there was little opportunity to trace the life cycle of a tropical cyclone and to study the wake of the storm and the dynamic effects of sea surface temperature upon the storm. But in order to at least show sea surface temperature values near a hurricane, a grid print map of orbit 246 was run off by the IBM 7094 computer. Figure 17 shows the T_{BB} analysis over Hurricane Gladys after it intensified beyond the tropical storm stage at 0334Z on 14 September 1964. The shaded sea area of "cool" 290° to $297^{\circ}K$ (63° to $75^{\circ}F$) values to the west of Gladys was probably covered by a cloud layer. The warm water (297° to $298^{\circ}K$), between 10° to $16^{\circ}N$, is approximately 5° to $6^{\circ}K$ colder than the climatological values indicated for the area in U. S. Navy Hydrographic Office Publication 225. This limited sea area is admittedly not of sufficient size to delineate the warm water tongues which could cause the intensification of a tropical storm. Satellite radiation coverage over the clearer subsidence region of annular zone on the outer limits of cirrus outflow of a mature storm may be the best area for satellite study of the sea surface temperature patterns. Low-level aircraft radiation flight surveys of the sea

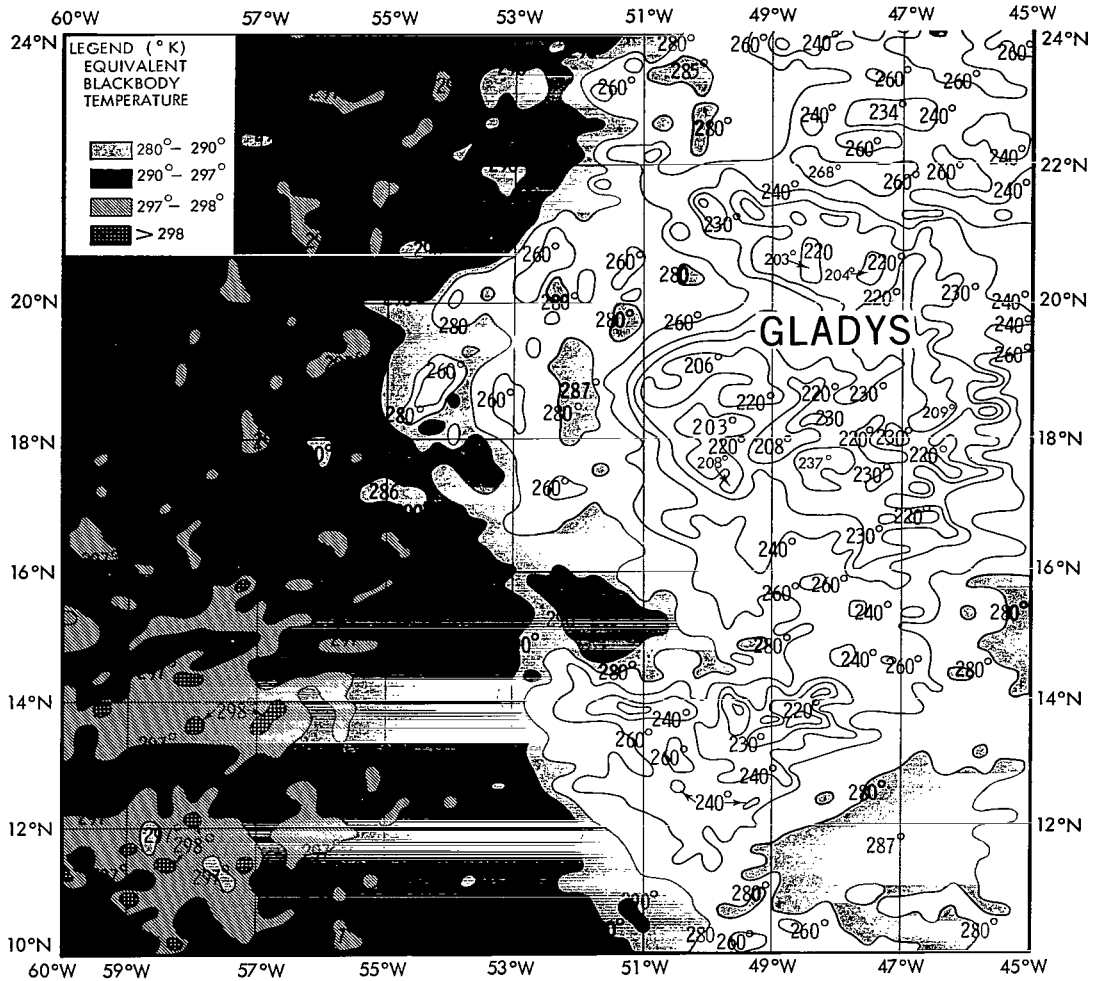


Figure 17—Analysis of HRIR T_{BB} values ($^{\circ}$ K) from Nimbus I orbit 246 R/O 247, 0334Z for 5 min., on 14 September 1964 near Hurricane Gladys in the subtropical Atlantic Ocean.

surface which avoid rain areas within 150 to 300 miles of the storm's center, could circumvent the cloud contamination problem.

The Middle East Maritime Region

By the middle of September 1964, the cloudy southwest monsoon had weakened considerably over the Indian Ocean. The Red Sea-Persian Gulf regions were near their maximum sea surface temperature. Owing to the arid climate and excessive evaporation in this area, the surface water salinity approached a high value. Theoretically, there should not be any appreciable surface emissivity difference detected by the satellite radiometer from open ocean waters of average salinity (32 to 37 parts per thousand) or from semi-enclosed waters of high salinity (up to > 40 parts per thousand) found in the Middle East region.

The Indian Ocean and Middle East were well-covered by overflights of Nimbus I and more than forty orbits were available for study. Figure 18 shows the analyzed HRIR sea surface temperature chart (T_{BB} in $^{\circ}\text{K}$) for orbit 300 over the Persian Gulf at 2009Z, 17 September 1964. This orbit was selected from 4 similarly located orbits because it contained the least cloud contamination and was well-centered over the Persian Gulf. T_{BB} values of 300° to 304°K (81° to 88°F) are shaded by darker greys for emphasis; the values of $<298^{\circ}\text{K}$ (77°F) were probably cloud-contaminated. Figure 19 shows the climatological sea surface temperature and sea current data for September as analyzed by the U. S. Naval Oceanographic Office, Physical Property Office (from unpublished data). The satellite T_{BB} values in the Persian Gulf and Gulf of Oman were found to be 2° to 6°K colder than the September climatological ship data.

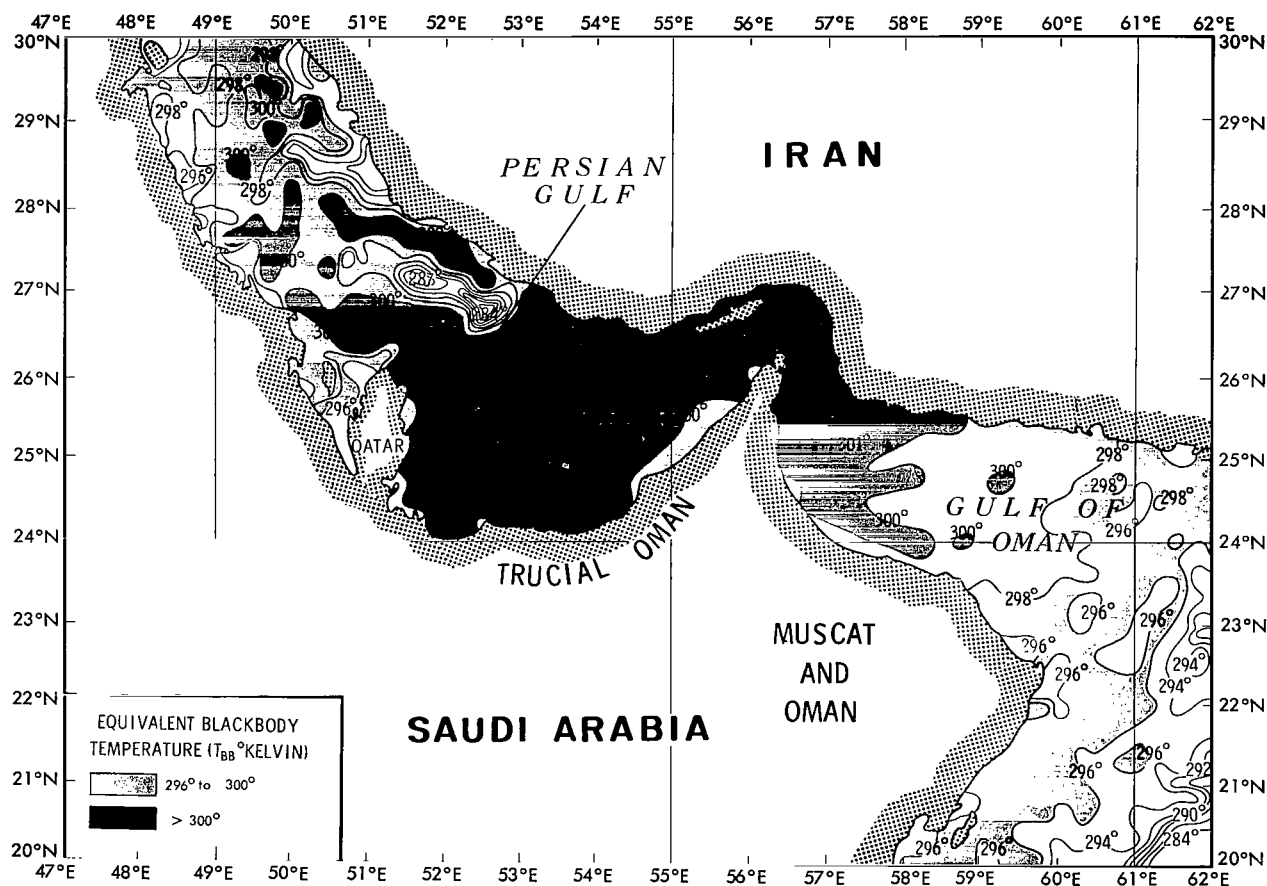


Figure 18—Analysis of HRIR T_{BB} values ($^{\circ}\text{K}$) from Nimbus I orbit 300 R/O 301, 2009Z for 8 min., on 17 September 1964 over the Persian Gulf.

Figure 20 shows orbit 37, recorded at 2037Z on 30 August 1964 and delineates the best available coverage of the Caspian Sea. The Caspian Sea is the largest shallow inland salt lake in the world. Sea surface temperature data were not available for this area. As a last resort, the 72°F (295°K) isotherm indicated over the shallow eastern portion of the Black Sea (Figure 19), which is

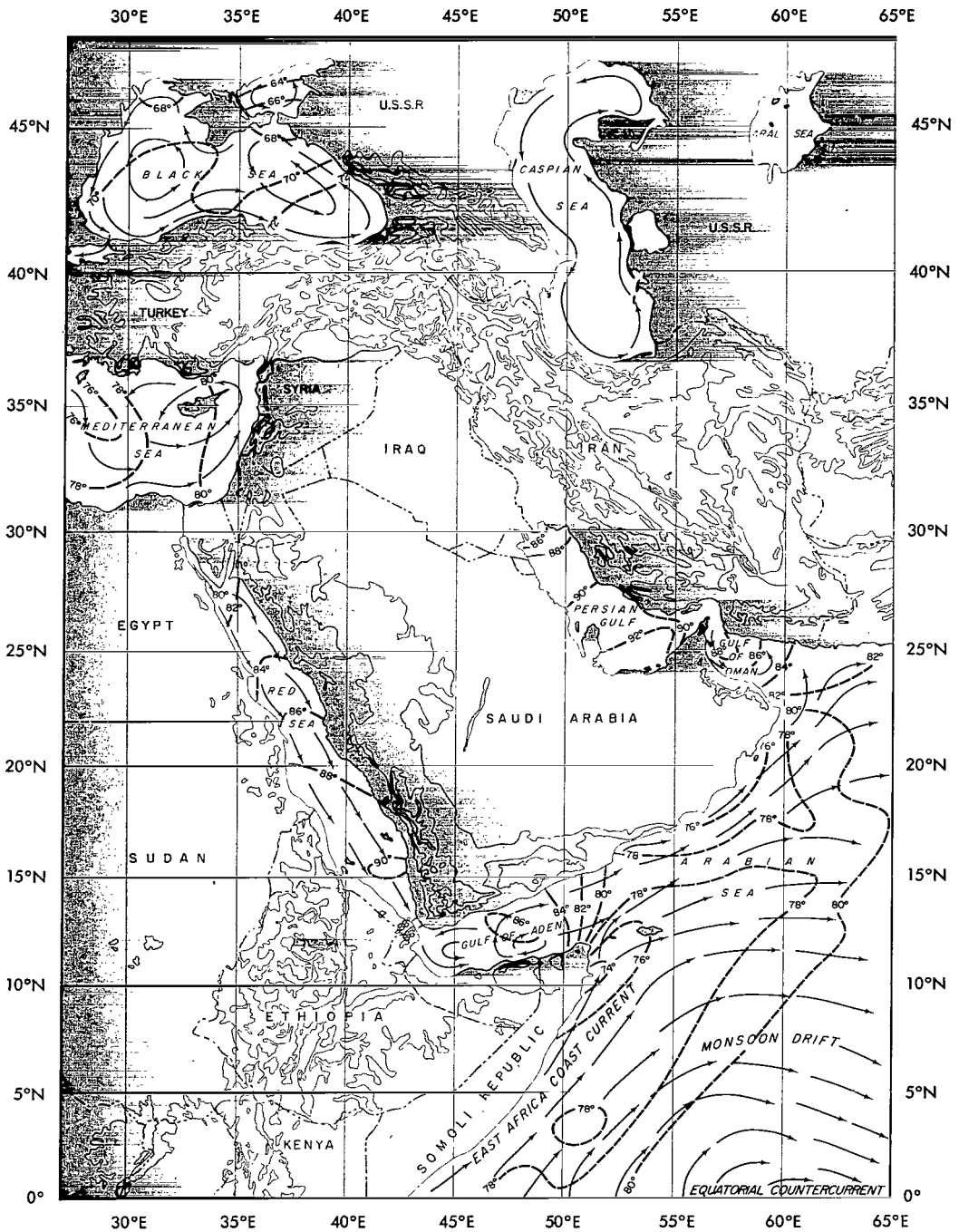


Figure 19—Climatological ship sea surface temperature (°F) and current chart analyzed by the U. S. Naval Oceanographic Office, Washington, D. C., for September in the Middle East.

at the same approximate latitude, was chosen for comparison. The darker shaded T_{BB} values of 292° to 294°K at 40° to 42°N were found to be 1° to 3°K cooler than the Black Sea climatological values.

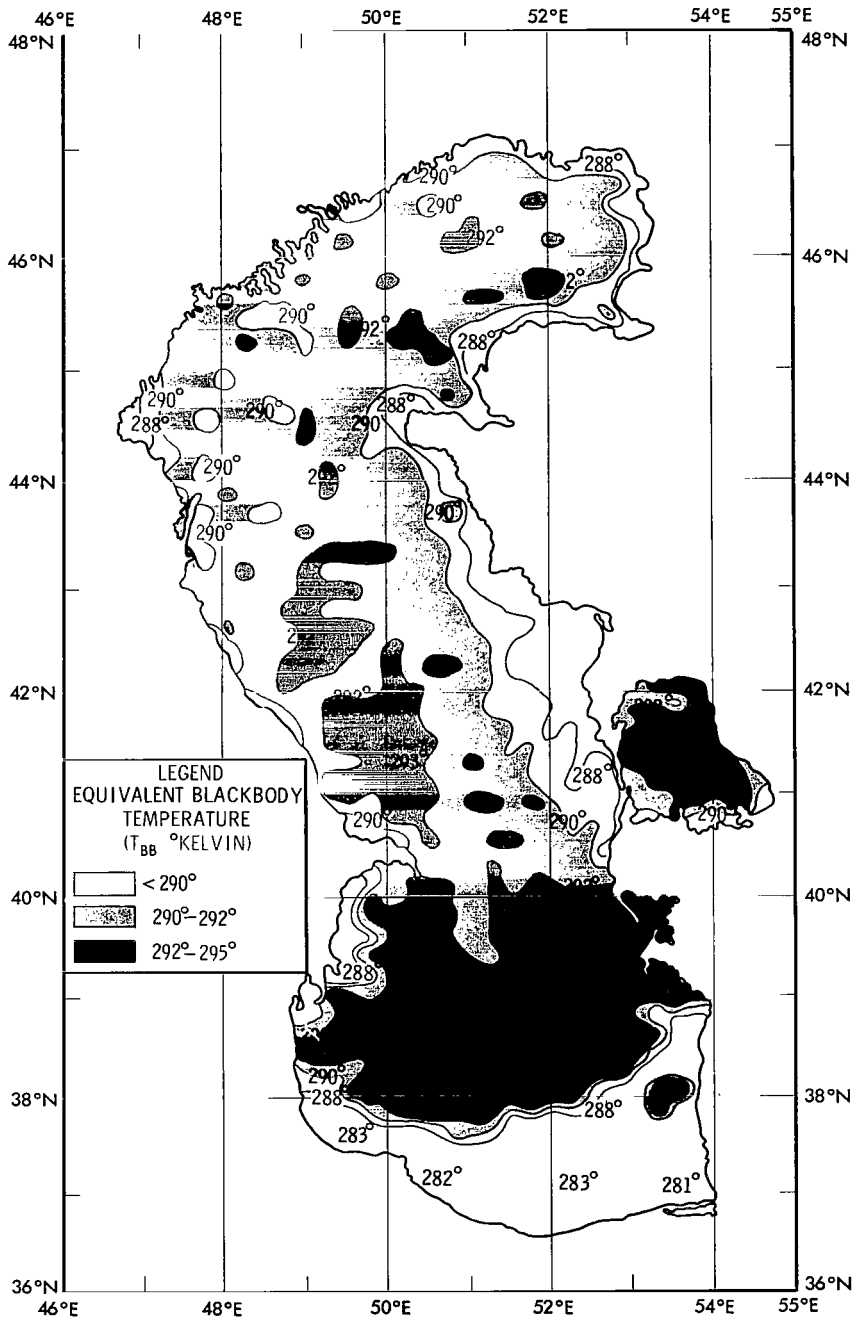


Figure 20—Analysis of HRIR T_{BB} values (°K) from Nimbus I orbit 037 R/O 038, 2037Z for 9 min., on 30 August 1964 over the Caspian Sea.



Figure 21—HRIR Photofacsimile chart of Nimbus I orbit 037 R/O 038 on 30 August 1964 over the Caspian Sea.

The cooler 281° to 290°K T_{BB} values along the eastern and southern shoreline are shown as a lighter grey stratoform cloudy area on the Nimbus photofacsimile picture of the same orbit (Figure 21).

Data over the eastern Mediterranean and Red Sea were recorded by orbit 345 at 2153Z on 20 September 1964. Figure 22 shows the T_{BB} analysis for this orbit. The 294°K T_{BB} values in the

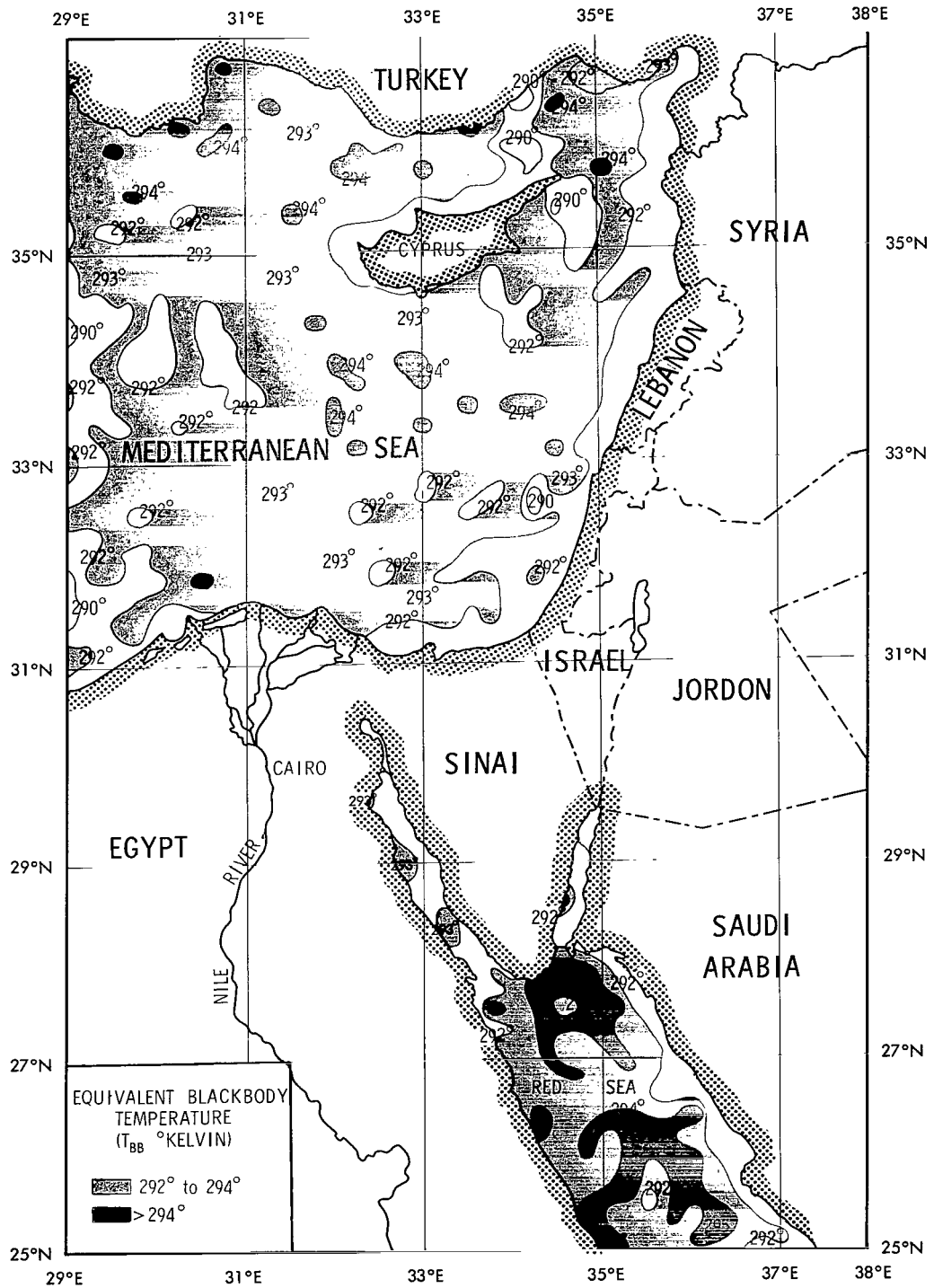


Figure 22—Analysis of HRIR T_{BB} values ($^{\circ}\text{K}$) from Nimbus I orbit 345 R/O 349, 2153Z for 8 min., on 20 September 1964 over the Eastern Mediterranean Sea and Red Sea.

vicinity of Cyprus, overlies the 80°F (300°K) climatological isotherm shown in Figure 19, and indicate a -6°K temperature difference. The areas of 290° to 292°K values were probably cloud covered. The Red Sea analysis indicates the T_{BB} values of 294° to 295°K which overlie the 80° to 83°F (300° to 301°K) climatological isotherms shown in Figure 19 and indicate a similar -6°K temperature difference.

Further to the southeast, data for the Somali coast were recorded by orbit 139 at 2002Z on 6 September 1964. Figure 23 shows the T_{BB} analysis for the orbit. The 296° to 297°K T_{BB} values in the entrance to the Gulf of Aden overlie the 84° to 86°F (302° to 303°K) climatological isotherms shown in Figure 19 and also indicate a -6°K temperature difference. The T_{BB} values <290°K from 9° to 12°N are related to the position of stratus and stratocumulus clouds located over the cold upwelled water off the Somali coast. This shallow current which flows southwest to northeast along

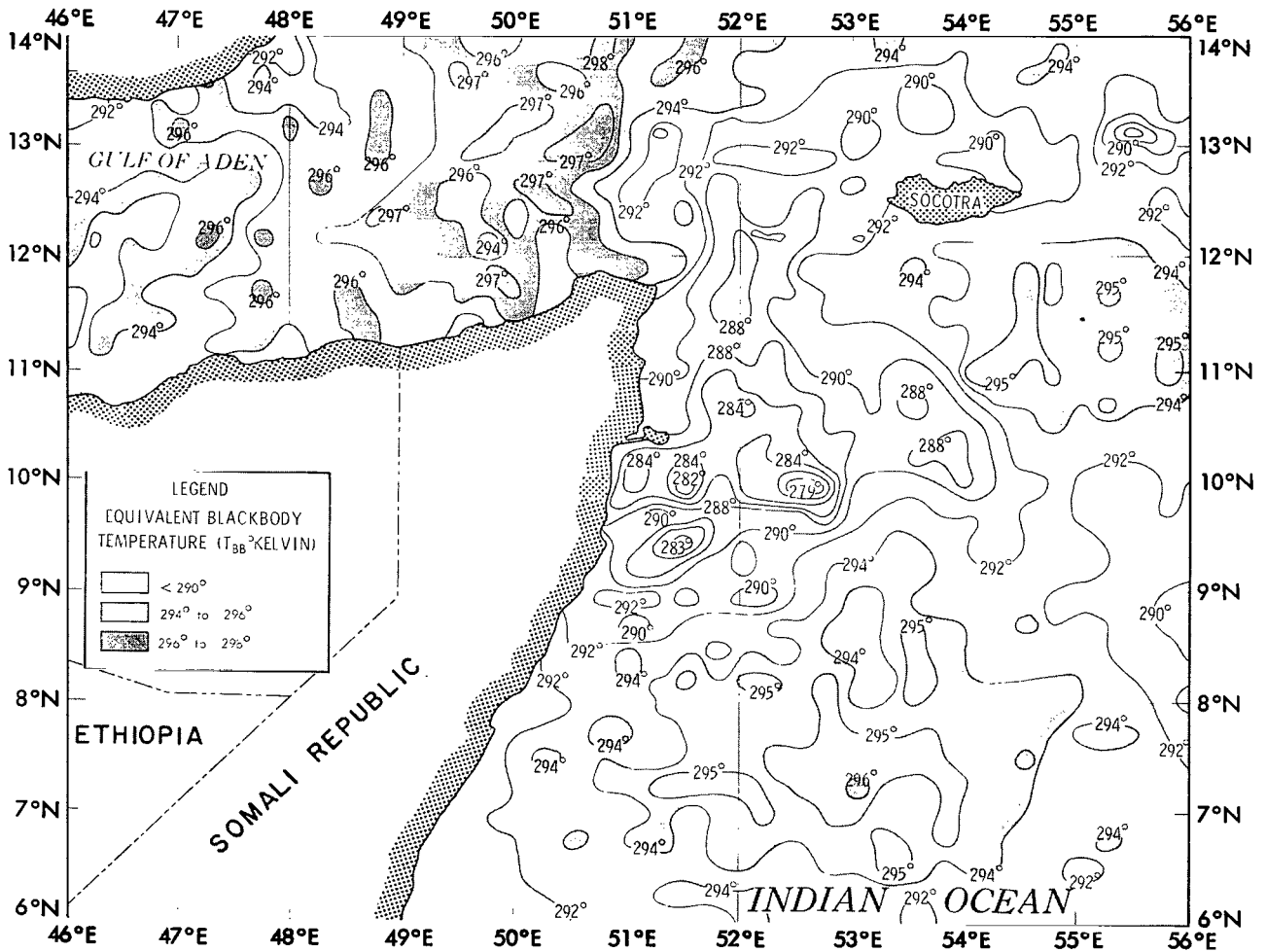


Figure 23—Analysis of HRIR T_{BB} values (°K) from Nimbus I orbit 139 R/O 140, 2002Z for 8 min., on 6 September 1964 over the Somali coast.

the African coastline, is driven by the winds of the southwest monsoon. The steep pressure gradient, (1017 mb to 997 mb) developed along the northeast coast of Africa, Saudi Arabia and India during this August-September period, causes the air to accelerate north of 5°N latitude, and a low level jet is produced (Reference 23). The sea-air interaction induces the Somali current to turn in a northeasterly direction over a coastal region which is very straight and steep and where the bottom topography is smooth. Marked upwelling of cold water, 13°C (286°K), was noted in a surrounding region of 24°C (297°K) isotherms by the research vessels ARGONAUT and DISCOVERY during their cruise in this area in August-September 1964 (Reference 23). A sea surface temperature analysis recorded during this expedition and analyzed by H. Stommel and B. Warren of the Woods Hole Oceanographic Institute is shown in Figure 24. The upwelled water, indicated by 14° to 22°C (287° to 295°K) sea surface isotherms, appears to underlie the cloudy region of cool T_{BB} values (279° to 290°K) shown in Figure 23. The shaded area of 294° to 296°K T_{BB} values from 6° to 9°N overlies the 22° to 24°C (295° to 297°K) sea surface isotherms and indicates a -1° to -3°K temperature difference.

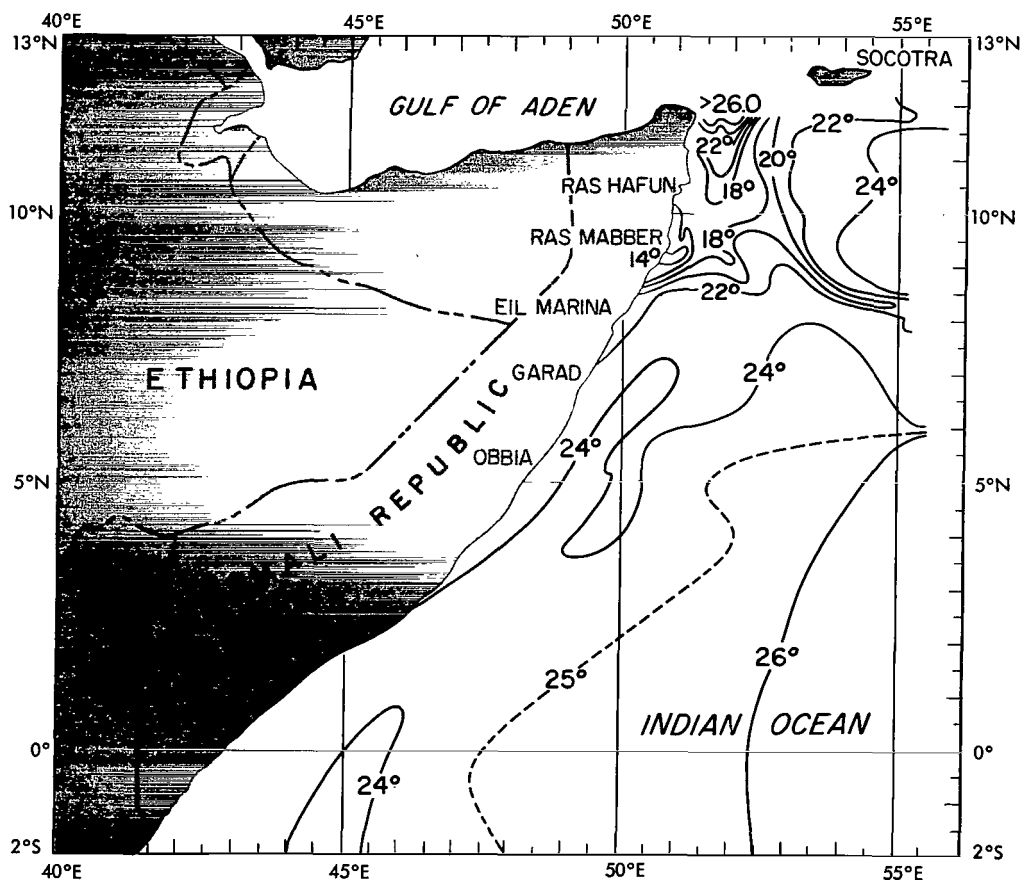


Figure 24—Oceanographic research ship sea surface temperature (°C) analyzed, by H. Stommel and W. Wooster August-September 1964.

CONCLUSION

This study of sea surface temperatures derived from Nimbus HRIR nighttime data, aircraft radiometer data, and conventional ship data indicates that the satellite radiometer is capable of collecting limited amounts of useful oceanographic data. Under certain synoptic conditions, when a cloud-free sea surface can be assumed, the derived sea surface temperature is noted to be 3° to 6°K colder than aircraft radiation measurements and synoptic-climatological ship sea surface temperature data. Even after correcting for atmospheric absorption, there is a residual 1° to 3°K uncertainty which is probably due to cloud cover. Future satellite instrumentation will include an HRIR radiometer sensitive in the 10-11 μ region to make daytime measurements. When used in conjunction with television data or a high resolution short wave radiometer (0.55-0.75 μ), this system could delineate 10 to 30 percent of the world's cloud free areas daily and derive sea surface temperatures from the corresponding 10-11 μ region.

ACKNOWLEDGMENTS

The authors wish to thank Mr. William R. Bandeen, Goddard Space Flight Center, for his helpful comments and suggestions in the review of this paper. We are particularly grateful to Mr. James H. Johnson, U. S. Bureau of Commercial Fisheries and Mr. John C. Wilkerson, Oceanographic Prediction Division, U. S. Naval Oceanographic Office for providing oceanographic data used in this study.

Goddard Space Flight Center
National Aeronautics and Space Administration
Greenbelt, Maryland, April 27, 1967
160-44-04-02-51

REFERENCES

1. Ewing, G. C., ed., "Oceanography from Space," Woods Hole Oceanographic Institution, Woods Hole, Mass., Ref. No. 65-10, April 1965.
2. Greaves, J. R., Wexler, R., and Bowley, C. J., "The Feasibility of Sea Surface Temperature Determination Using Satellite Infrared Data," ARACON Geophysics Co., Concord, Mass., Final Report 9G16-F, November 1965.
3. Sattinger, I. J., and Polcyn, F. C., "Peaceful Uses of Earth Observation Spacecraft," Vols. I, II, and III, Willow Run Laboratories, University of Michigan, Ann Arbor, Michigan, February 1966.
4. Ewing, G. C., "The Outlook for Oceanographic Observations from Satellites," in *Proceedings of the Third Symposium on Remote Sensing of the Environment*, Oct. 14-16, 1964, University of Michigan, Ann Arbor, Michigan, February 1965.

5. Clark, J., ed., "Techniques for Infrared Survey of Sea Temperature," Bureau of Sport Fisheries and Wildlife, Dept. of Interior, Bureau Circular References No. 202, November 1964.
6. Foshee, L. L., Goldberg, I. L., and Catoe, C. E., "The High Resolution Infrared Radiometer (HRIR) Experiment," in *Observations from the Nimbus I Meteorological Satellite*, NASA SP-89, 1965.
7. Kunde, V. G., "Theoretical Relationship between Equivalent Blackbody Temperatures and Surface Temperatures Measured by the HRIR," in *Observations from the Nimbus I Meteorological Satellite*, NASA SP-89, 1965.
8. Wormser, E. M., "Measurement of Ocean Surface Temperatures," Appendix B, pp. 381-393, in *Fundamentals of Infrared Technology*, MacMillan Co., New York, N. Y., 1962.
9. Ewing, G., and McAlister, E. D., "On the Thermal Boundary Layer of the Ocean," *Science* 131:1374-76, 1960.
10. Ewing, G. C., "Slithering-Isotherms and Thermal Fronts on the Ocean Surface," Techniques for Infrared Survey of Sea Temperature, Clark, J., ed., Dept. of Interior Circular 202, November 1964.
11. Staff Members, "Nimbus I High Resolution Radiation Data Catalog and Users' Manual," Vol. 1, Photofacsimile Film Strips, p. 226, Goddard Space Flight Center, Greenbelt, Md., January 15, 1965.
12. Potocsky, G., Kniskern, F., "Report of Severe Ice Conditions in Melville Bugt, Summer 1964," Unpublished Manuscript Report No. 0-53-65, pp. 45, Marine Sciences Dept., U. S. Naval Oceanographic Office, Washington, D. C., March 1966.
13. Saur, J. F. T., "A Study of the Quality of Sea Water Temperatures Reported in Logs of Ships' Weather Observation," *Journal of Applied Meteorology* 2(3):417-425, 1963.
14. Namias, J., "Air-Sea Interaction," McGraw Hill Yearbook of Science and Technology, 1965.
15. Blackburn, M., "Oceanography and the Ecology of Tunas," *Oceanogr. Mar. Biol. Ann. Rev.* 3:299-322, 1965.
16. Mariners Weather Log, U. S. Dept. of Commerce, *ESSA*, 10(3):82, May 1966.
17. Stewart, H. B., Jr., Zetler, B. D., and Taylor, D. B., "Recent Increases in Coastal Water Temperature and Sea Level - California to Alaska," U. S. Dept. of Commerce, Coast and Geodetic Survey, Technical Bulletin, No. 3, 1958.
18. Leipper, D., "The Gulf of Mexico after Hilda," *Sea-Air Interaction Laboratory Report No. 1*, pp. 163-184, Technical Note 9-Sail-1, Sea-Air Interaction Laboratory, ESSA, U. S. Dept of Commerce, August 20, 1965.

19. Fisher, E. L., "Hurricanes and the Sea Surface Temperature Field," Part I, National Hurricane Research Project, Report No. 8, 1957.
20. Perlroth, I., "Intensity of Hurricanes in Relation to Sea Surface Energy Exchange," pp. 147-161, *Sea-Air Interaction Laboratory Report No. 1*, Technical Note 9-Sail-1, Sea-Air Interaction Laboratory, ESSA, U. S. Dept. of Commerce, August 20, 1965.
21. Jordan, C. L., "Evidence of Surface Cooling Due to Typhoons," *Sea-Air Interaction Laboratory Report No. 1*, pp. 187-190, Technical Note 9-Sail-1, Sea-Air Interaction Laboratory, ESSA, U. S. Dept. of Commerce, August 20, 1965.
22. O'Brien, J. J., and Reid, R. O., "On Upwelling in a Two-layer Baroclinic Ocean Induced by Momentum Transfer from a Stationary, Axially-Symmetric Hurricane," Paper presented at *47th Annual AGU Meeting*, April 19-22, 1966.
23. Bunker, A. F., "A Low Level Jet Produced by Air, Sea and Land Interactions," *Sea-Air Interaction Laboratory Report No. 1*, pp. 225-238, Technical Note 9-Sail-1, Sea-Air Interaction Laboratory, ESSA, U. S. Dept. of Commerce, August 20, 1965.

"The aeronautical and space activities of the United States shall be conducted so as to contribute . . . to the expansion of human knowledge of phenomena in the atmosphere and space. The Administration shall provide for the widest practicable and appropriate dissemination of information concerning its activities and the results thereof."

—NATIONAL AERONAUTICS AND SPACE ACT OF 1958

NASA SCIENTIFIC AND TECHNICAL PUBLICATIONS

TECHNICAL REPORTS: Scientific and technical information considered important, complete, and a lasting contribution to existing knowledge.

TECHNICAL NOTES: Information less broad in scope but nevertheless of importance as a contribution to existing knowledge.

TECHNICAL MEMORANDUMS: Information receiving limited distribution because of preliminary data, security classification, or other reasons.

CONTRACTOR REPORTS: Scientific and technical information generated under a NASA contract or grant and considered an important contribution to existing knowledge.

TECHNICAL TRANSLATIONS: Information published in a foreign language considered to merit NASA distribution in English.

SPECIAL PUBLICATIONS: Information derived from or of value to NASA activities. Publications include conference proceedings, monographs, data compilations, handbooks, sourcebooks, and special bibliographies.

TECHNOLOGY UTILIZATION PUBLICATIONS: Information on technology used by NASA that may be of particular interest in commercial and other non-aerospace applications. Publications include Tech Briefs, Technology Utilization Reports and Notes, and Technology Surveys.

Details on the availability of these publications may be obtained from:

SCIENTIFIC AND TECHNICAL INFORMATION DIVISION
NATIONAL AERONAUTICS AND SPACE ADMINISTRATION
Washington, D.C. 20546